HELICAL PILES IN SOFT SENSITIVE SOILS – A FIELD STUDY OF DISTURBANCE EFFECTS ON PILE CAPACITY

Christopher N. Weech, M.A.Sc., P.Eng.,
Thurber Engineering Ltd., Victoria, B.C., Canada

John A. Howie, Ph.D., P.Eng.,
University of British Columbia, Vancouver, B.C., Canada

ABSTRACT Small diameter helical auger piles can be installed in locations with restricted access and limited headroom and are frequently an attractive alternative for underpinning of existing structures. They may also be a practical alternative to conventional driven piles for new structures. A field study was undertaken to examine the performance of these piles in lightly overconsolidated, sensitive clayey silt in South Surrey, B.C. Piezometers were installed at selected depths and at several radii from the pile center prior to pile installation to allow monitoring of the variation in pore pressures with distance from the pile during and after pile installation and during load testing. The test piles were instrumented with strain gauges to measure load distribution and pore pressure transducers to monitor pore pressures at the pile wall after installation and during load testing. The piles were load tested to failure at 1 day, 1 week and 6 weeks after installation. The paper presents results of field monitoring of pore pressures created by installation and test loading and will present the load test results. Mobilized soil shear strengths back-calculated from load tests at different times after installation are compared to natural and remoulded shear strengths measured using in-situ tests. The implications of these results on the selection of appropriate shear strength parameters for use in design and on the prediction of the length of the recovery period after installation are discussed.

Introduction to Helical Piles

Helical piles consist of a series of helix-shaped circular plates that are attached to a slender steel shaft. The helices, which are typically fixed to a lead shaft section of up to 3 m length, can all have a common diameter or the helices may increase in diameter with distance above the tip of the pile. The shaft sections are typically comprised of either hollow steel pipe or solid steel square bar. The piles are installed by rotating the shaft using a hydraulic torque unit. The helices cut downward into the soil thereby pulling the shaft into the ground. Shaft extensions, which are typically either 1.5 m or 3 m in length, are added via bolted connections as the pile is advanced into the ground, until the desired bearing depth is reached. The piles can be installed using relatively small and lightweight equipment and in conditions of low overhead clearance. Consequently, this type of pile has been used frequently in recent years for repairs and retrofits of existing foundations. As the volume of soil displaced by this type of pile is limited to the volume of the slender steel shaft and the thin helix plates, helical piles can be classified as “low-displacement” piles.

These installations have been widely used as tensioned soil anchors and for foundations to resist large overturning moments because of their efficiency in resisting uplift forces. When helical piles are used to support compression loads, the slender shafts can be prone to buckling before the full geotechnical capacity of the helical plates can be mobilized. To minimize the potential for buckling, the shaft can be encased in a column of cement grout. Vickars Developments Co. Ltd. of Burnaby, B.C. patented a method of forming the grout column during installation using discs that are located at the bottom of each extension section. The annular cavity formed behind the disc is kept full with grout during the entire pile installation process. This adaptation of the more conventional ungrouted helical pile design has been registered under the trademark PULLDOWN™ Pile.

Helical piles are usually screwed into some competent bearing stratum at relatively shallow depth. There are many areas, however, where the depth to a competent bearing stratum makes it more economical to install shorter friction piles rather than longer end-bearing piles. There has been relatively little experience using helical piles as friction piles in soft fine-grained soils.

This paper summarizes the results of a field research program investigating the performance of PULLDOWN™ Piles in a soft sensitive clayey silt in Surrey, B.C. The objectives of the research were to improve the understanding of the effects of installation disturbance and subsequent recovery on the capacity of this configuration of helical piles in such soils.

UBC Helical Pile Research

At the time of testing, it was standard practice to space helices at 3 plate diameters regardless of the type of soil in which the pile was installed. Narasimha Rao et al. (1993) suggested that for helices spaced at greater than about 2 plate diameters, capacity is mobilized by the helices individually in end-bearing; while at helix spacing-to-diameter ratios (S/D) of 1.5 or less, the soil fails along a cylindrical surface defined by the outer edge of the helices. Their research also showed that greater capacities can be mobilized in soft clays by anchors with S/D = 1.5 or less.

When installing helical piles within soft, fine-grained deposits, minimal torque is required for installation so the bearing area of the helix plates can be maximized. Thus, for this study, a uniform helix diameter (D) of 356 mm was selected for all of the plates, instead of the more common

configuration of plate diameter increasing with distance from the tip. Half of the piles had 5 plates spaced at 1.5 D, while the other half had 3 plates spaced at 3.0 D, such that the total length between the top and bottom helix was 2.1 m for all piles. The shaft consisted of steel pipe with an 89 mm outside diameter (O.D.) and with a closed-ended tip that was bevelled at 45°. The helix to shaft diameter ratio of this configuration was 4.0. The geometry of the test piles is shown on Fig. 1.

The hole for installation of the grout column was formed by 150 mm diameter discs located at the bottom of each extension. In order to minimize the contribution of the upper 2.5 m thickness of variable surficial soils to the overall pile capacity, a twin-walled PVC casing system was designed to isolate the upper 3 m shaft extension from friction due to the soil that is in contact with the outer casing. The only contact between the inner and outer casing was limited to a length of 25 mm where a PVC reducer sleeve was in contact with the base of inner PVC casing. The annular space between the pile shaft and the inner casing was filled with grout.

A total of 26 push-in electric piezometers were installed within the soil surrounding the 6 test piles prior to pile installation. The piezometers were installed at various depths and radial distances from the pile shaft. The radial distances of the piezometer filters from the center of the pile shaft after pile installation were determined by measuring the horizontal deviation of both the piezometer pipes and the pile shaft using a miniature inclinometer probe.

Electric pore pressure transducer ports and strain gauges were also mounted on the shaft of the test piles at the locations indicated on Fig. 2 (PP refers to piezo-ports, SG to strain gauges and TP to test piles). The cables containing the wires for the strain gauges and pore pressure transducers were run up the inside of the pile shaft. Pore pressures at the piezometers surrounding the piles and at the piezo-ports on the pile shaft were

Fig. 1. Test Pile Geometry

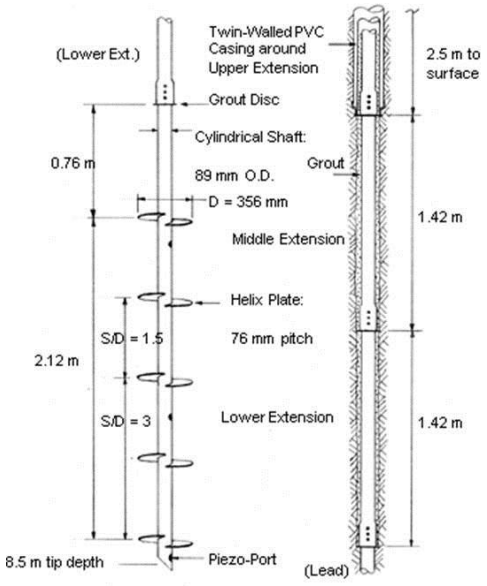

monitored during pile installation and during the subsequent dissipation period. The response of the soil during and after pile installation was described in Weech and Howie (2001).

Test piles were loaded to failure under axial compressive loads in accordance with ASTM Standard D1143 (Quick Load Test Method). Recovery periods after installation ranged from 19 hours to 6 weeks. Strain gauges mounted on the pile shaft were monitored during load testing to determine the distribution of loading throughout the pile at the various load levels up to and including failure. The piezometers and piezo-ports were also monitored during load testing since the distribution of excess pore pressures can be used as an indicator of the distribution of soil deformations caused by pile displacement. This paper deals with the effect of disturbance during pile installation and the subsequent recovery process on the measured pile capacities.

Test Site

The site is located under the south end of the Highway 99A overpass over Colebrook Road in the Serpentine River Lowland area of Surrey, B.C., 2.5 km east of the sea at Mud Bay. A detailed in-situ site characterization program was carried out prior to installing the test piles. The subsurface information gathered during this study supplemented previous data obtained by Crawford & Campanella (1991), as well as available data obtained by the Ministry of Transportation and Highways and published by Crawford & deBoer (1987).

Fig. 2. Locations of Strain Gauges and Piezo-ports on Test Piles

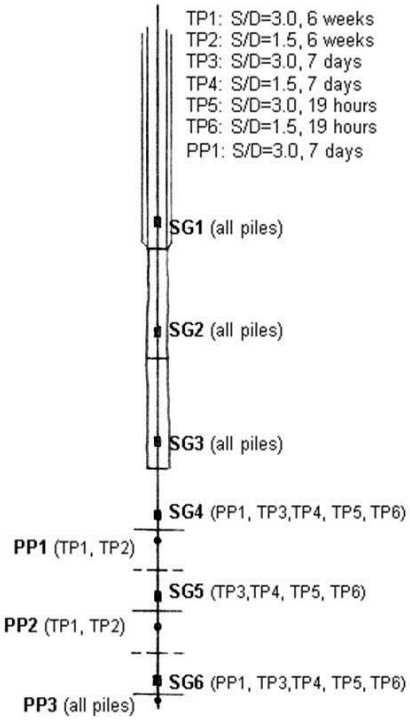

The ground surface at the site lies below sea level, varying between –1.1 m and –1.3 m elevation. The test site is covered with a 0.5 m to 0.7 m thickness of fill material overlying a 0.2 m to 0.3 m thickness of peat, which formed the original ground surface. The peat is underlain by a layer of clayey silt interlayered with seams of fine sand to sandy silt which extends to about –3.2 m elevation (2m depth). The surficial soils are underlain by an extensive deposit of deltaic clayey silt overlying marine silty clay, which extends to about 25 m depth. This research programme focussed on the more uniform clayey silt from –4 m to –10 m elevation. These fine-grained soils are inferred to be post-glacial Fraser *River* sediments of the Quaternary period, which were laid down at the mouth of the Fraser River between 10,000 and 5,000 years ago (Dolan, 2001).

Measured plasticity indices (IP = w_{LL} - w_{PL}) ranged from 8% to 21%, with an average of 13.5%. The natural water content averaged 42% (standard deviation of 4%) below -3.7 m elevation (~2.5 m depth). Higher water contents were measured above this elevation due to the presence of fibrous organics within the soil. The natural water content was typically above the liquid limit of the soil, with measured liquidity indices (IL) typically between 1 and 2.

Piezometers located within the upper 10 m of the soil indicated that the water table is typically around –2 m elevation (~0.8 m below ground level) and that there is an upward hydraulic gradient which is typically between 5% and 10%. This upward gradient is likely due to groundwater recharge from the upland area just north of the site, by way of the more permeable sand and gravel underlying the marine deposit at about 25 m depth.

Salt contents of 14 to 15 g/L and 11 to 12 g/L were measured from samples above and below –6.8 m (~5.6 m depth), respectively. These salt contents are less than half the typical depositional salt content of marine clays, which indicates that some leaching has occurred, likely as a result of the upward flow of groundwater at the site.

In-Situ Testing Programme

Piezocone penetration test (CPTu) soundings were carried out at the research site using three different cone penetrometers with tip load cell capacities ranging from 0.4 to 10 tonnes and with pore pressure elements at different locations. Pore pressure measurements during penetration were obtained at the u_1, u_2 and u_3 locations on the penetrometers. The u_1 position is midway up the cone face, u_2 is the standard position behind the shoulder of the cone, and u_3 is behind the friction sleeve.

Typical results of the CPTu soundings are presented on Fig. 3, including:

- tip resistance corrected for pore pressure effects (q_t),
- friction ratio ($R_f = f_s/q_t$, where f_s is the sleeve friction measurement and R_f is quoted as a percentage),
- excess pore pressure ratio ($B_q = \Delta u_2/(q_t-\sigma_{vo})$, where Δu_2 is the excess pore pressure generated during cone penetration and σ_{vo} is the total overburden pressure.

Shear wave travel times were measured at depth intervals of both 0.5 m and 1.0 m using a seismic module located above the friction sleeve on the cone penetrometer (SCPT). Shear wave velocities (V_s) calculated from the measured shear wave travel times according to the interval method described by Robertson et al. (1986) are also presented on Fig. 3.

A Nilcon field vane boring apparatus was used to obtain a profile of in-situ undrained field vane shear strength, $(s_u)_{FV}$, as well as remoulded shear strength, $(s_u)_{rem}$. This apparatus includes a slip coupling located between the vane and rods that allows the measured torque to be corrected for the effects of rod friction. The peak and remoulded shear strengths measured during the field vane shear tests (FVST) are also plotted on Fig. 3. The sensitivity (S_t) of the fine-grained soils, as measured by the ratio of peak to remoulded $(s_u)_{FV}$ values, increases with depth from a minimum of 6 to a range of 14 to 20 below -6.8 m elevation (~5.6 m depth).The high sensitivity, generally high liquidity, and the low salt contents are further evidence that the fine-grained soil at this site has a metastable microstructure, possibly due to leaching by fresh water after salt-water deposition. Site-specific values of N_{kt} were calculated from the equation $N_{kt} = (q_t-\sigma_{vo})/(s_u)_{FV}$. An average N_{kt} of 11.6 was obtained, with a standard deviation of 2.0. This value was used to generate continuous profiles of $(s_u)_{FV}$ with depth as shown in Fig. 4. Continuous profiles of $(su)_{FV}$ normalized by the effective overburden pressure (σ'_{vo}), are also shown on Fig. 4.

The $(s_u)_{FV}/\sigma'_{vo}$ ratio decreases with depth, indicating that overconsolidation ratio (OCR) diminishes with depth. Values of OCR were calculated from the CPTu data and from the $s_u)_{FV}/\sigma'_{vo}$ profiles using a number of published methods (Sully et al. 1990; Ladd et al. 1977; Schmertmann 1978; Chen and Mayne 1995; Mayne 1991 and 1992).The OCR profiles on Fig. 4 show the range of calculated values, with the maximum and minimum values discarded, for each of three different CPT locations. There is a moderately overconsolidated crust between –4 m and –5 m elevation (3.8 to 4.8 m depth) that may be due to desiccation during a time when this part of the deposit was exposed at ground surface. Below this crust, the OCR generally ranges from 2 to 3 above –9 m (7.8 m depth) and from 1 to 2 below –9 m (7.8 m depth), indicating that the clayey silts within the depth range of interest in this study are lightly overconsolidated. The CPTu q_t profiles increase linearly with depth below about -8.2 m (17 m depth) suggesting that the soil may be normally consolidated below this depth. However, extrapolation of this linear trend to ground surface suggests that light overconsolidation continues below 17 m depth. This apparent overconsolidation within the deposit is very common in the Lower Fraser Valley lowland areas and is inferred to be a product of the microstructure of these soils, rather than from actual geologic precompression.

Pore pressure dissipation tests with simultaneous measurements of pore pressure at the u_2 and u_3 positions were carried out at different depths, including one test that lasted 8.4 hours. Values of the coefficient of horizontal consolidation, c_h, estimated from CPTu dissipation tests were relatively consistent with depth, with an average of 0.019 cm^2/s (standard deviation of 0.005 cm^2/s).

Fig. 3. Typical CPTu and SCPTu Profiles at the site

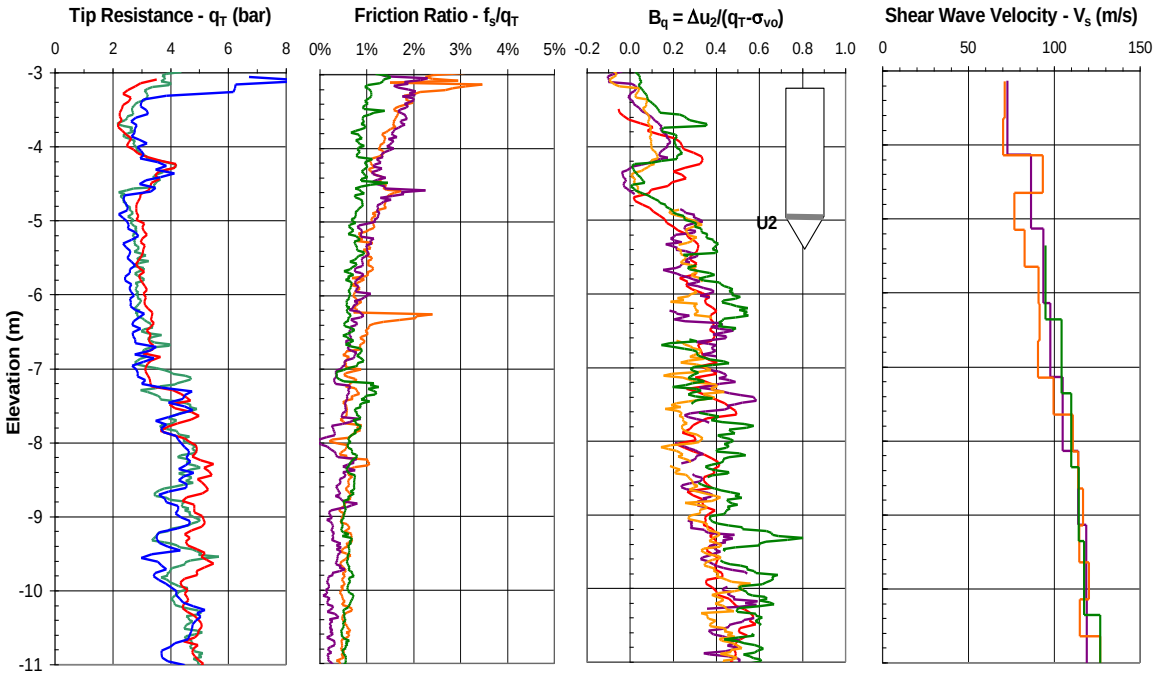

Fig. 4. Profiles of Measured and Estimated $(s_u)_{FV}$, $(s_u)_{FV}/\sigma'_{vo}$ and OCR Profiles

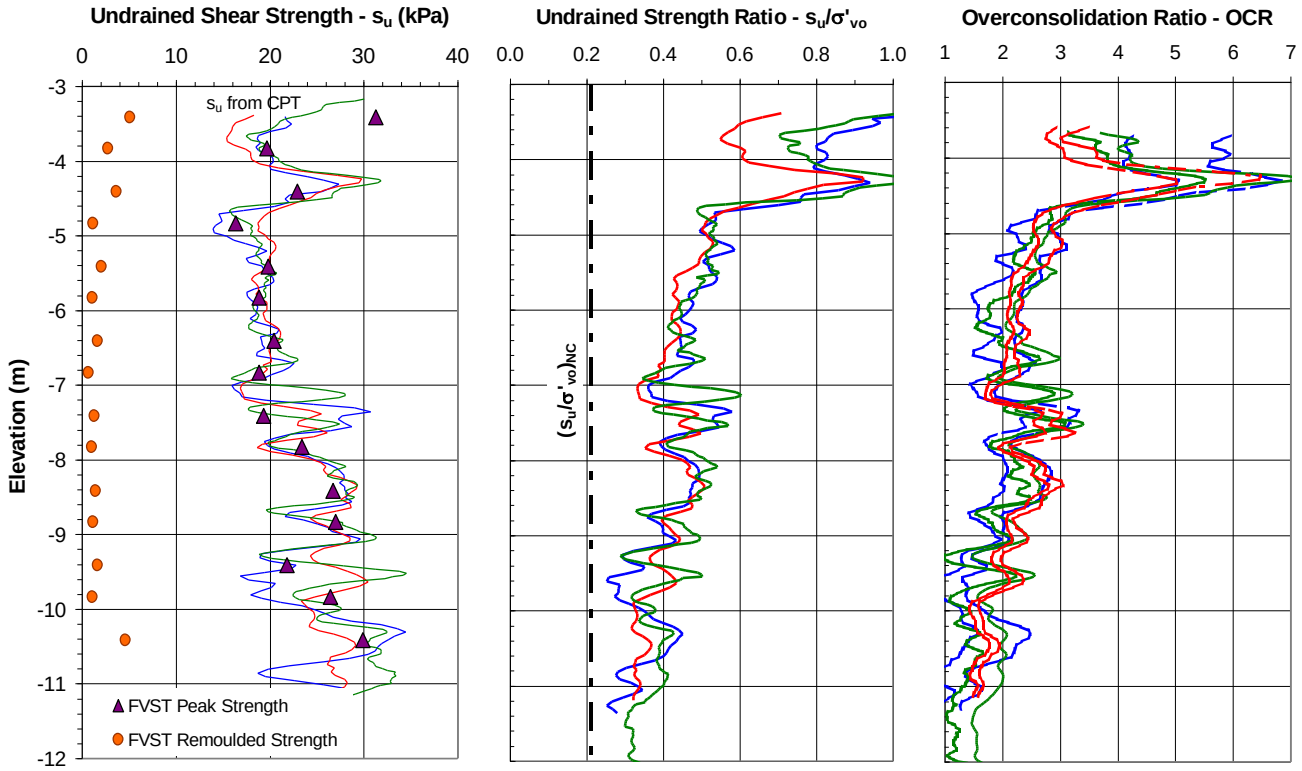

Soil Response to Pile Installation

The pore pressure response at and around the piles during installation is described in Weech and Howie (2001). A very sudden increase in pore pressure was observed at the piezometers located within 8 radii of the pile center as the tip of the pile shaft passed the filter elevation of the piezometer. This initial increase is inferred to be a result of the soil deformation caused by penetration of the tip of the pile shaft, which was approximately 15 cm long below the bottom helix. The initial sudden increase was followed by an additional increase as the bottom helix plate passed the piezometer filter elevation.

After this peak, the piezometers within $r/R_{shaft} = 8$ exhibited a trend of decreasing $\Delta u/\sigma'_{vo}$ with continuing penetration, with very little response to the passing of subsequent helices. At the piezometers beyond $r/R_{shaft} = 8$, the pore pressure was observed to build up gradually with continuing penetration of the pile, reaching a maximum magnitude and then remaining roughly constant as successive plates passed the level of the piezometers. These observations suggest that only the soil located within a radial distance of about 10 to 12 times the plate thickness from the edge of the helix plates responds directly to the penetration of the plates. However, there appeared to be a gradual outward propagation of Δu during continuing pile penetration, which occurred more quickly than can be explained by pore water flow. The magnitude of excess pore pressure generated within the soil by the pile installation decreased with radial distance from the pile.

The radial distributions of $\Delta u/\sigma'_{vo}$ for locations above the bottom helix plate at various times after stopping installation are plotted on Fig. 5. Excess pore pressure can be observed out to a distance of almost 100 R_{shaft} immediately after stopping pile installation ($\Delta u \geq 0.1\sigma'_{vo}$ out to r/R_{shaft} of around 60 at 0.1 minutes after stopping). The radial extent of elevated pore pressures was found to be less for piezometers below the level of the bottom helix plate. The radial distribution of $\Delta u/\sigma'_{vo}$ generated by helical pile installation at the Colebrook test site extended to greater radius than the distribution induced by penetration of the shaft alone as indicated by the dashed line on Fig. 5). The dissipation of pore pressure around the piles was monitored after installation and the change in distribution with time is shown in Fig. 5.

For all of the test piles, the dissipation of excess pore pressure was essentially complete at around 10,000 minutes, or about 7 days, for most locations around the piles. No significant differences were observed in the dissipation rates between the piles with S/D=1.5 and S/D=3. From observation of pore pressure dissipation, it was observed that the time to 90 percent dissipation at the pile shaft below the bottom helix, was about 1.5 to 2.5 times shorter than that recorded on the shaft between the helices. Pore pressure observations suggest that greater disturbance is caused as the spacing of the helices decreases and that the extent of disturbance and rate of pore pressure dissipation is less beneath the bottom helix than above.

Fig. 5. Radial Distribution of Excess Pore Pressures around Piles During Dissipation Process

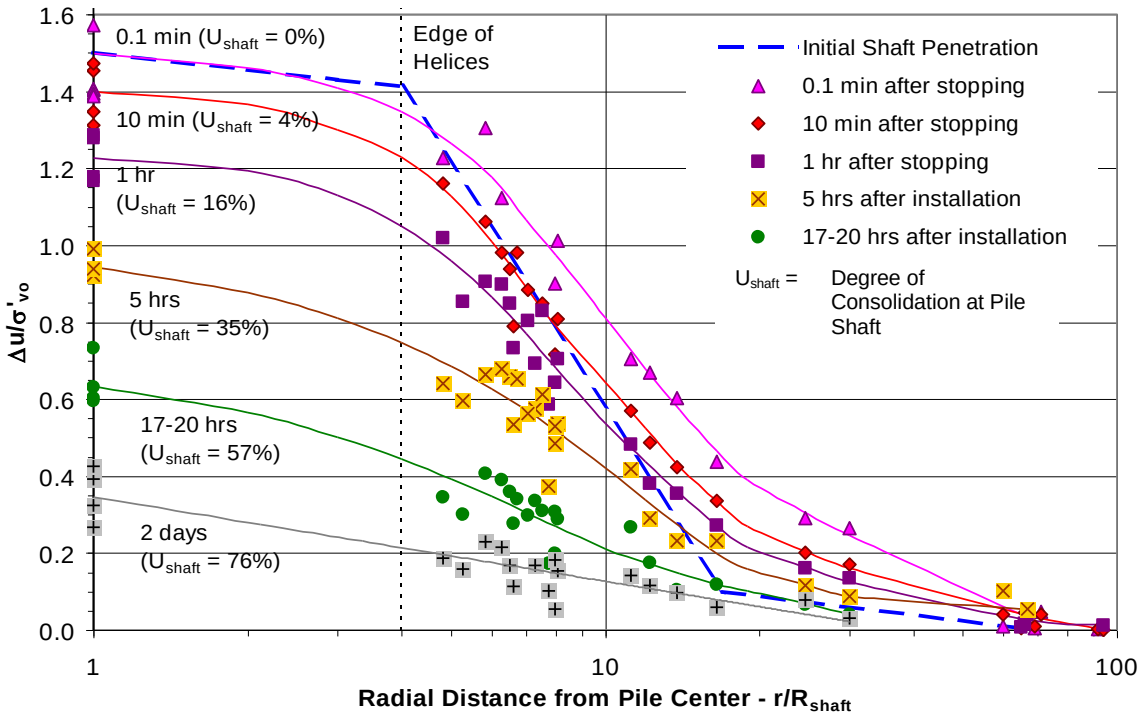

Load Testing and Observed Mobilization of Pile Resistance

Load tests were carried out on different piles at 19 hours, 7 days, and 6 weeks after installation. At 19 hours, pore pressure dissipation was 60% to 70% complete within the soil surrounding the helices. The tests at 7 days corresponded to the end of the dissipation period. Load testing was conducted in general accordance with the setup and procedures specified as the "Quick Load Test Method for Individual Piles" in the ASTM Standard D1143. Details of the specific setup and procedures used are provided in Weech (2002).

Plots of total pile load versus pile head displacement are presented in Fig. 6. The pre-failure points on these curves correspond to the settlements measured at the end of each load interval (after the load had been maintained for about 5 minutes).

The initial response of the pile to loading is quite stiff. As a result, the measured movements at 50% of pile capacity are quite small: about 4 to 6 mm (1.2 to 1.5 percent of D_{hx}) at 7 days and 6 weeks, and 6 to 8 mm (1.7 to 2.2 percent of D_{hx}) at 19 hours. At load levels closer to failure, the movement of the S/D=3 piles is noticeably greater than that of the S/D=1.5 piles. Failure of all of the piles was characterized by rapid plunging.

Capacities ranged from 63 to 68 kN at 19 hours after installation to 80 to 90 kN at 6 weeks. The S/D=1.5 piles had the least capacity at 19 hours and the largest at 6 weeks and so exhibited a significant increase in capacity over that time period compared to the S/D=3 piles.

The pile strain gauges made it possible to estimate the initial load in the piles prior to testing and the distribution of resistance mobilized by the various distinctive sections of the piles for each increment of loading. Fig. 7 illustrates how the distribution of load mobilized by the various sections of pile TP6 varied during the loading test.

Table 1 provides a summary of the pile capacities and indicates the relative contributions to the total capacity of the lead section and the grouted column above the lead. For five piles, it was also possible to estimate the relative contributions of the bottom helix and the upper helices as shown in the table.

Fig. 6. Load Test Results

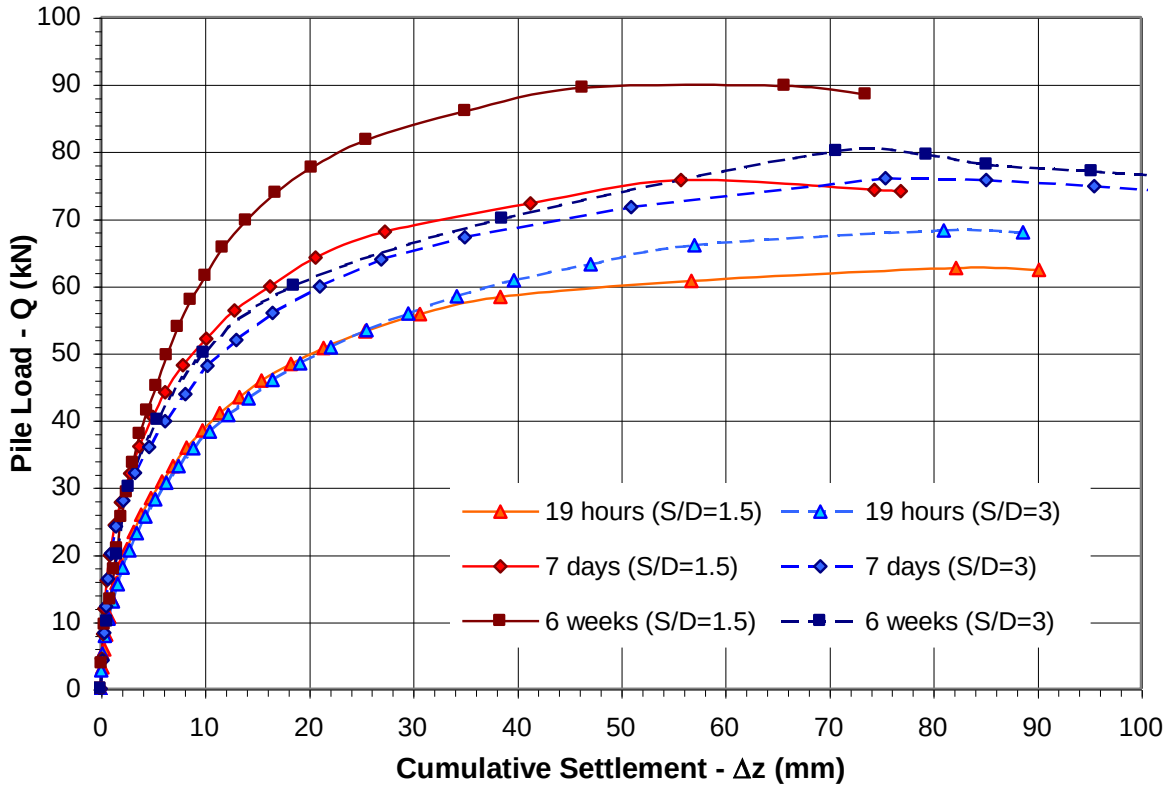

Fig. 7. Distribution of Load in Pile TP6.

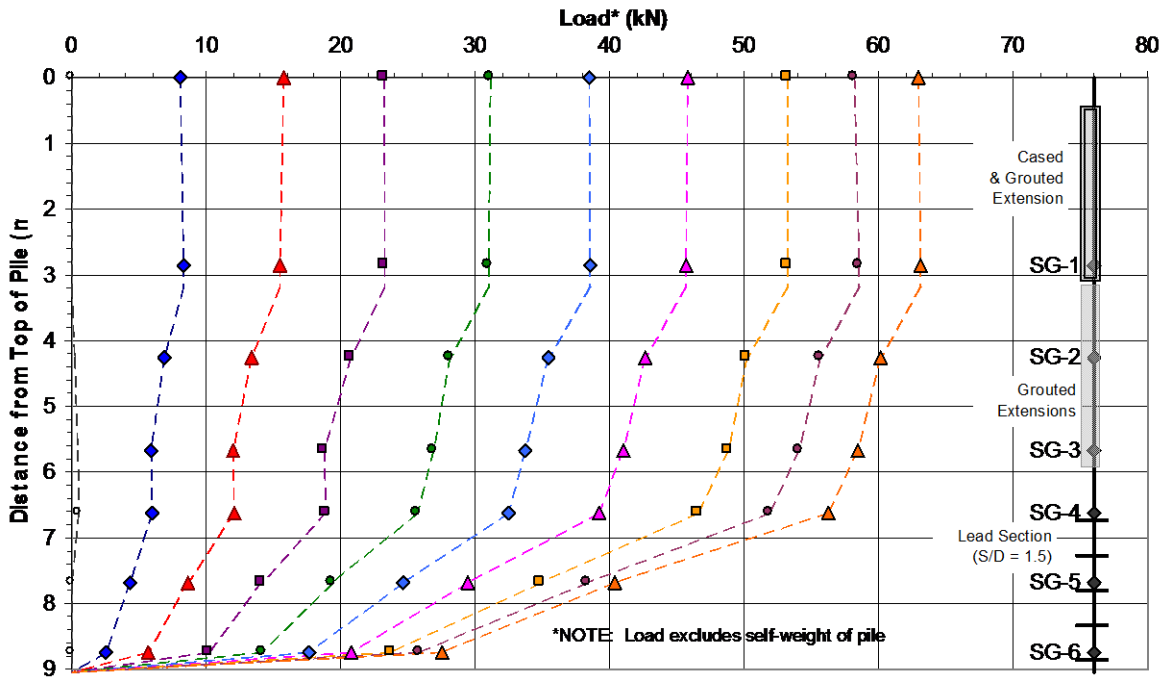

Table 1. Mobilized Soil Resistance at Pile Failure

Pile No.	Helix S/D	Recovery Time (days)	Soil Resistance[1] (kN) at Failure				
			Pile Total	Grout Column[2]	Lead Section[3]	Upper Helices[4]	Bottom Helix[5]
TP5	3	0.8	68.5	5	63.5	35.5	28
TP3	3	7	76	14	62	33.5	28.5
PP1	3	7	77	14	63	37	26
TP1	3	42	80				
TP6	1.5	0.8	63	6.5	56.5	29	27.5
TP4	1.5	7	76	15	61	38	23
TP2	1.5	43	89.5				

Notes:
(1) loads rounded to the nearest 0.5 kN
(2) from bottom of casing to SG4 (entire grout column, incl. bottom grout disc)
(3) from SG4 to pile tip (i.e. all helices)
(4) from SG4 to SG6 (i.e. all helices except bottom plate)
(5) below SG6 (i.e. bottom plate and tip of shaft)

Discussion

Rational methods of calculating helical pile capacity based on soil shear strengths and/or bearing capacity factors have been developed. Two distinct methods have been proposed: the “cylindrical shear method” and the “individual plate bearing method”. In the cylindrical shear method, a continuous cylindrical failure surface extending between the top and bottom helix plates is assumed to form along the perimeter of the helix plates. In the individual plate bearing method, individual bearing failures are assumed to occur above (pile in uplift) or below (pile in compression) each helix plate.

Extensive research carried out on model helical piles at the Indian Institute of Technology (IIT) in Madras, India (Narasimha Rao et al., 1989, 1991, 1993), has revealed that the spacing of the helix plates has an important influence on the failure mechanism. This testing was carried out in tanks that were filled with very soft, completely remoulded clay of known moisture content and shear strength measured using the vane shear test. In these tests, a nearly continuous cylindrical failure surface was observed after the piles were pulled out of the clay when the helix plate spacing (S) was set to 1.5 plate diameters (D), i.e. S/D=1.5. At an S/D ratio of 2.3 and greater, clay remained on the top of the plates, but a continuous cylindrical failure surface did not develop.

The IIT research showed that the capacity of helical piles installed in fine-grained soils can be predicted with a good degree of accuracy using the undrained shear strength (s_u) of the soil, provided that an appropriate value for this parameter is known. The IIT results suggest that the best accuracy is achieved using the cylindrical shear method to predict the capacity (Q_{cyl}) of helix plates at S/D $\leq$ 1.5 according to the following equation:

[1] $$Q_{cyl} = \pi D \cdot L_{cyl} \cdot s_u$$

where L_{cyl} is the length between the top and bottom helix plate. For 16 pile tests in both uplift and compression, a mean over-prediction of 5%, with a standard deviation of 5%, was achieved (Narasimha Rao et al., 1991).

They also found that the capacity (Q_b) of helices spaced at S/D > 2 could be predicted with a reasonable degree of accuracy using the *individual plate bearing method,* typically resulting in underestimation of up to 20% according to Narasimha Rao et al., 1993. The following equation is used in this method:

[2] $Q_b = \Sigma(A_{hx} \cdot N_c \cdot s_u)$

where A_{hx} is the bearing area of each helix plate and N_c is an empirical bearing capacity factor, which is typically assumed to be around 9 for deep foundations subjected to undrained loading.

In the tests reported here, pore pressures around the piles were monitored during load testing. Radial distributions of Δu at pile failure normalized by the effective overburden pressure at the start of the test (i.e. $\Delta u_f/\sigma'_{vo}$), generated by the bottom helix and the upper (top and middle) helices of both S/D=1.5 and S/D=3 piles, are compared directly on Fig. 8. The variation of Δu with radius measured by the piezometers indicates that the zone of soil that is loaded by the upper helices on the S/D=1.5 piles only extends out to between $r/R_{helix} = 1.5$ and 2 (about 14 cm beyond the edge of the helices). By comparison, it appears that the soil loaded by the upper helices on the S/D=3 piles extends out to about $r/R_{helix} = 3$, while the soil loaded by the bottom helix extends out beyond $r/R_{helix} = 4$.

The limited radial extent of Δu generated by the upper helix plates at S/D = 1.5 is consistent with the pattern of soil deformations that would be expected for cylindrical shearing. The greater extent of soil deformations caused by the loading of the bottom helix plate and the upper plates at S/D = 3 is consistent with the failure mechanism caused by individual plate bearing. This is consistent with observations of pile behaviour where it typically requires more pile movement to mobilize end bearing resistance than frictional resistance. It is thus possible to analyze the test results based on the following assumptions:

- that the failure mechanism for the S/D=3 piles is by individual bearing failure at each helix
- that the failure mechanism for the S/D=1.5 piles is by individual bearing failure for the bottom helix and that the upper part of the pile fails along a cylindrical failure surface of the same diameter as the helices.

Fig. 8. Radial Distributions of Excess Pore Pressure Generated at Pile Failure

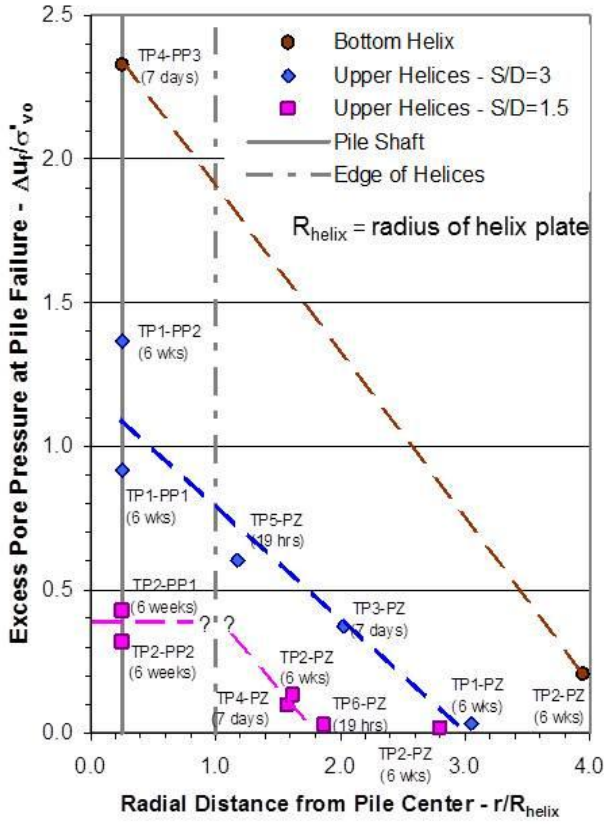

The average bearing pressures at failure induced by the bottom helix plates and by the upper helices at S/D = 3 (Δq_f) are plotted on Fig. 9, along with the profiles of net tip resistance, $q_{net} = q_t - \sigma_{vo}$, measured in the intact soil at three different CPTu locations prior to pile installation.

Below each data point representing Δq_f from the piles, a vertical bar extends to a distance of 2 helix diameters to represent the likely zone of greatest bearing influence from the helix plates. The calculated bearing pressures below the bottom helix (helix plate and pile tip) are very close to the range of q_{net} pressures for 6 out of 7 of the test piles (all except TP4). This figure suggests that q_{net} from the CPTu test can be used for estimation of the resistance mobilized by the bottom helix but that a reduced value is applicable to the estimation of the capacity of the upper helices. This is most likely due to the destructuring of the soil that was caused by the helices during pile installation.

Equations 1 and 2 were used to back-calculate the average undrained shear strength mobilized by the various sections of the piles, $(s_u)_{pile}$, from the known loads transferred to the soil at failure. These back-calculated shear strengths are compared to profiles of peak (intact) and remoulded undrained shear strengths interpreted from the FVST and CPTu data on Fig. 10. The profiles of peak $(s_u)_{FV}$ from CPTu data indicate the variability in natural soil strength at the site. The frictional resistance measured by the friction sleeve on the cone penetrometer, f_s, and an inferred profile of normally consolidated s_u for the test site are also plotted on Fig. 10. The vertical bars above and/or below each data point representing $(s_u)_{pile}$ indicate the approximate vertical extents of the zones over which the average $(s_u)_{pile}$ is inferred to apply.

For the grout column, the average values of $(s_u)_{pile}$ that are plotted on Fig. 10 correspond to the peak resistance mobilized at pile movements of between 2 mm and 10 mm. The residual strengths that were determined at pile failure after movements in excess of 45 mm were typically between 8 and 8.5 kPa for most of the piles tested at 7 days and 6 weeks (TP3 was slightly lower). This is very close to the strength plotted for Pile TP4 which did not show any peak in strength, and to the average normally consolidated shear strength for that depth interval.

Fig. 9. Helix Bearing Pressure at Pile Failure Compared to q_{net} from CPTu

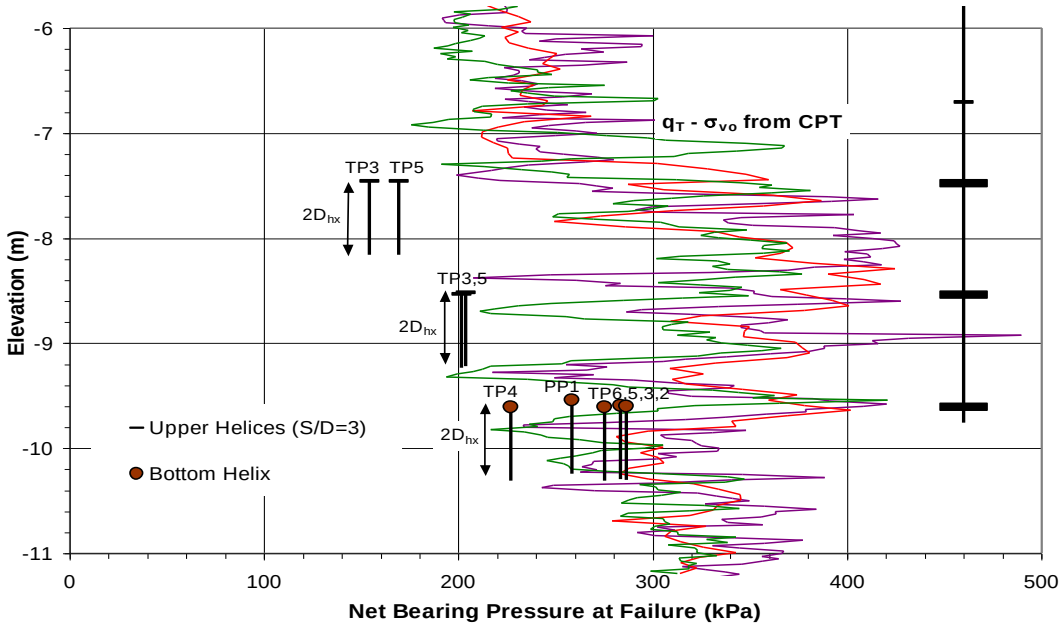

Fig. 10. Undrained Shear Strengths Mobilized by Piles Compared to In-Situ Strength Measurements

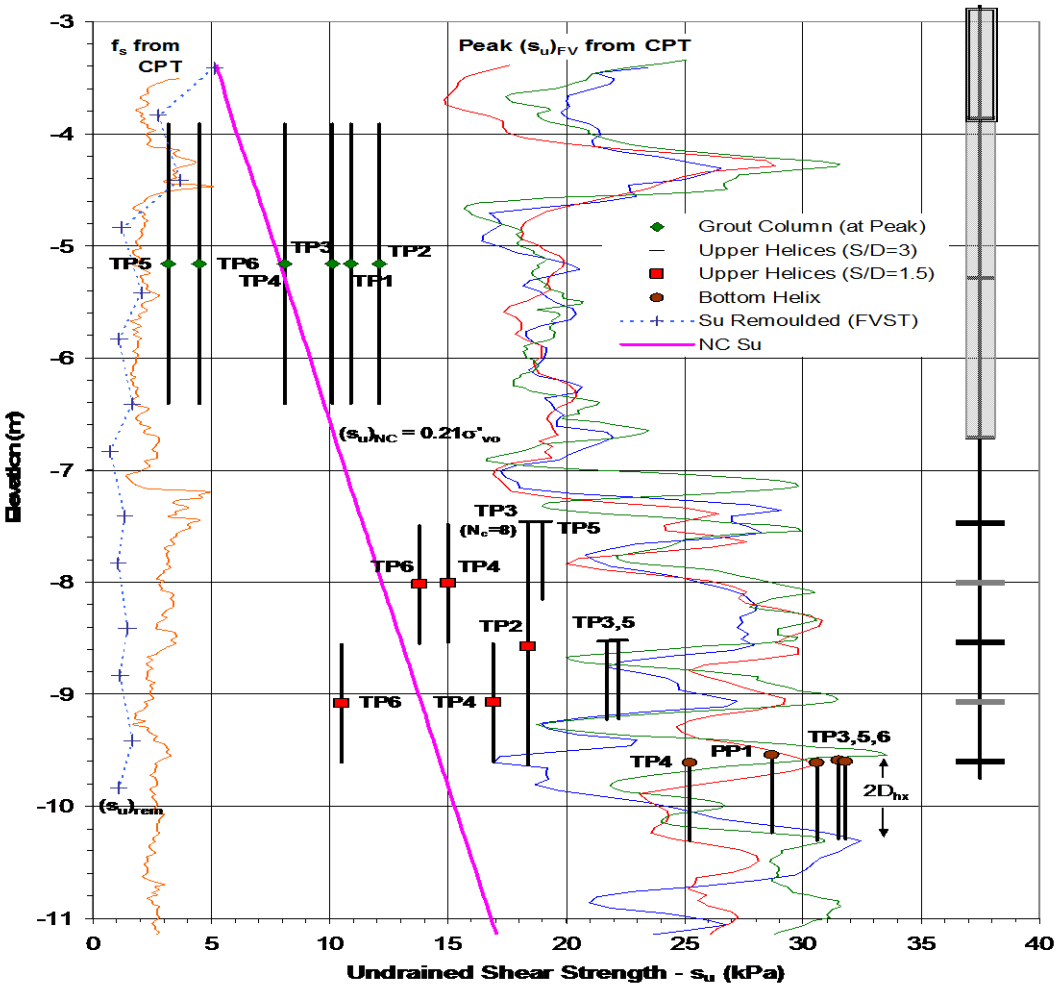

It is apparent from Fig. 10 that the peak s_u measured within the intact soil would not be appropriate for predicting the capacity of the piles, except for below the bottom helix. The pile installation process has clearly caused a reduction in shear strength within the soil above the bottom helix, likely as a result of soil destructuring, which persists long after the dissipation of excess pore pressure is complete.

The degree to which the destructuring has affected the mobilized strength appears to vary for the different pile sections, as follows:

Grout Column: The peak s_u mobilized along the surface of the grout column at 19 hours is only slightly greater than the remoulded strength of the soil. The available strength then increases with time, but is still significantly less than the intact $(s_u)_{FV}$ of the soil before pile installation as a result of the very severe destructuring induced by the grout plates during pile installation;

Upper Helices (S/D = 1.5): s_u mobilized by the upper four helix plates increases with time during the pore pressure dissipation period and continues to increase after dissipation is complete. Five weeks after the end of the dissipation period, s_u is less than the peak $(s_u)_{FV}$ of the soil prior to pile installation. This reduction in shear strength is attributed to significant destructuring caused by pile installation. However, unlike for the grout column, the shear strengths mobilized at 19 hours do not suggest that the soil near the edge of the helices was completely remoulded during pile installation;

Upper Helices (S/D = 3): The undrained shear strength mobilized by the upper two helix plates is close to but consistently less than the peak $(s_u)_{FV}$ at similar elevations, at both 19 hours and 7 days (no change with time). This indicates that soil disturbance close to the pile shaft and between the helices has a more limited effect on the capacity mobilized by the more widely spaced plates. This is probably due to the fact that shearing must occur through a significant volume of soil beyond the edge of the helices during a bearing-type failure, and much of this soil may not have experienced any significant structural breakdown during installation.

Bottom Helix: The undrained shear strengths mobilized by the bottom helix plates (assuming $N_c = 9$) are at or slightly greater than the peak $(s_u)_{FV}$ at similar elevations. Clearly, the effect of installation disturbance on the strength available below the piles is negligible.

Conclusion

This paper has presented the results of observations of pore pressures during and after installation of helical piles and interpretation of load test results on these piles in a soft, sensitive clayey silt. The results have shown that helical piles with S/D=1.5 have higher capacities than for S/D=3 in soft clays. The results have confirmed the applicability of the design approach that assumes that the failure mechanism changes as the S/D ratio of the helices reduces. In this case study, it appeared that the failure mechanism for piles with S/D=3 is by individual bearing failure at each helix, whereas for piles with S/D=1.5, it is by individual bearing failure for the bottom helix and by shearing along a cylindrical failure surface of the same diameter as the helices for the remainder of the lead section.

The results also show that the undrained shear strength mobilized by helical piles in fine-grained soils is unlikely to be equivalent to the shear strength of the soil prior to pile installation, unless the soil is normally consolidated and unstructured prior to pile installation. The installation of the helical piles used in this study caused significant disturbance of the soil. However, the soil below the pile tip, which is loaded by the bottom helix, is essentially intact after pile installation.

The capacity mobilized by the S/D=1.5 helices increases substantially with time as the shear strength of the soil surrounding the piles recovers after pile installation. This is because the cylindrical failure surface induced by the S/D=1.5 helices passes through soil that has been softened and destructured by pile installation. Consequently, care should be taken to load test such piles after dissipation of excess pore pressure is substantially complete. Conversely, the capacity of the S/D=3 helices does not appear to increase significantly with time after installation and so the effect of installation disturbance is less. This is believed to be due to the bearing-type failures induced by the S/D=3 helices which mobilize resistance from a significant volume of soil beyond the edge of the helices, much of which does not appear to have experienced any significant softening or structural breakdown during installation.

Acknowledgements

The authors wish to thank Hubbell Power Systems for their financial support and for manufacturing and delivering the test piles, Vickars Development Co. for installing the piles and providing the infrastructure and manpower for the test site set-up, and ConeTec Investigations Ltd. for assisting with the in-situ testing. The assistance of the technical staff and the graduate students in the geotechnical group at the University of British Columbia is also greatly appreciated. The first author would also like to thank the Natural Sciences and Engineering Research Council of Canada for their financial support.

References

ASTM Standard D1143, Standard Test Methods for Deep Foundations Under Static Axial Compressive Load, ASTM International, West Conshohocken, PA, 2003, DOI: 10.1520/D1143_D1143M-07, www.astm.org.

Chen, B.S. and Mayne, P.W. 1995. Type 1 and 2 Piezocone Evaluations of Overconsolidation Ratio in Clays. Proceedings of CPT'95, Linköping, SGF Report 3:95, Vol. 2, pp. 143-148.

Crawford, C.B. and Campanella, R.G. 1991. Comparison of Field Consolidation with Laboratory and In Situ Tests. Canadian Geotechnical Journal, Vol. 28, pp. 103-112.

Crawford, C.B. & deBoer, L.J. 1987. Field Observations of Soft Clay Consolidation in the Fraser Lowland. Canadian Geotechnical Journal, Vol. 24, pp. 308-317.

Dolan, K. 2001. An in-depth Geological and Geotechnical Site Characterization Study, Colebrook Road Overpass, Highway 99A, Surrey, B.C. B.A.Sc. Thesis, University of British Columbia, Vancouver.

Ladd, C.C., Foott, R., Ishihara, K., Schlosser, F. and Poulos, H.G. 1977. Stress Deformation and Strength Characteristics. Proceedings of the 9th International Conference on Soil Mechanics and Foundation Engineering, Tokyo, Vol. 2, pp. 421-494.

Mayne, P.W. 1991. Determination of OCR in Clays by PCPT using Cavity Expansion and Critical State Concepts. Soils and Foundations, Vol. 31, No. 2, pp. 65-76.

Mayne, P.W. 1992. Closure, Determination of OCR in Clays by PCPT using Cavity Expansion and Critical State Concepts. Soils and Foundations, Vol. 32, No. 4, pp. 190-192.

Narasimha Rao, S., Prasad, Y.V.S.N., Shetty, D.M. and Joshi, V.V. 1989. Uplift Capacity of Screw Pile Anchors. Geotechnical Engineering, Vol. 20, No. 2, pp. 139-159.

Narasimha Rao, S., Prasad, Y.V.S.N., and Shetty, D.M. 1991. The Behaviour of Model Screw Piles in Cohesive Soils. Soils and Foundations, Japanese Society of Soil Mechanics and Foundation Engineering, Vol. 31, No. 2, pp. 35-50.

Narasimha Rao, S., Prasad, Y.V.S.N., and Veeresh, C., 1993. Behaviour of Model Screw Anchors in Soft Clays. Geotechnique, Vol. 43, pp. 605-614.

Robertson, P.K., Campanella, R.G., Gillespie, D.G. and Rice, A., 1986. Seismic CPT to Measure In-Situ Shear Wave Velocity. Journal of Geotechnical Engineering, ASCE, Vol. 112, No. 8, pp. 791-803.

Schmertmann, J.H. 1978. Guidelines for Cone Penetration Test Performance and Design. Federal Highways Administration, Report FHWA TS-78-209, Washington D.C.

Sully, J.P., Campanella, R.G. and Robertson, P.K. 1990. Overconsolidation Ratio of Clays from Penetration Pore Pressures. Journal of Geotechnical Engineering, ASCE, Closure, Vol. 116, No. 2, pp. 340-342.

Weech, C.N. 2002. Installation and Load Testing of Helical Piles in a Sensitive Fine-Grained Soil. M.A.Sc. Thesis, University of British Columbia, Vancouver, 223 p.

Weech, C. and Howie, J.A. 2001. Helical piles in soft sensitive soil – disturbance effects during pile installation. Proceedings of 54th Canadian Geotechnical Conference, Calgary, Alberta. pp. 281-288.